Weyl Points on Nonorientable Manifolds

André Grossi Fonseca,[1,*,†] Sachin Vaidya,[1,*,‡] Thomas Christensen,[2] Mikael C. Rechtsman,[3] Taylor L. Hughes,[4] and Marin Soljačić[1]

[1]*Department of Physics, Massachusetts Institute of Technology, Cambridge, Massachusetts 02139, USA*
[2]*Department of Electrical and Photonics Engineering, Technical University of Denmark, Kongens Lyngby 2800, Denmark*
[3]*Department of Physics, The Pennsylvania State University, University Park, Pennsylvania 16802, USA*
[4]*Department of Physics and Institute for Condensed Matter Theory, University of Illinois at Urbana-Champaign, Urbana, Illinois 61801, USA*

(Received 16 December 2023; revised 1 April 2024; accepted 3 May 2024; published 26 June 2024)

Weyl fermions are hypothetical chiral particles that can also manifest as excitations near three-dimensional band crossing points in lattice systems. These quasiparticles are subject to the Nielsen–Ninomiya "no-go" theorem when placed on a lattice, requiring the total chirality across the Brillouin zone to vanish. This constraint results from the topology of the (orientable) manifold on which they exist. Here, we ask to what extent the concepts of topology and chirality of Weyl points remain well defined when the underlying manifold is nonorientable. We show that the usual notion of chirality becomes ambiguous in this setting, allowing for systems with a nonzero total chirality. This circumvention of the Nielsen–Ninomiya theorem stems from a generic discontinuity of the vector field whose zeros are Weyl points. Furthermore, we discover that Weyl points on nonorientable manifolds carry an additional $\mathbb{Z}_2$ topological invariant which satisfies a different no-go theorem. We implement such Weyl points by imposing a nonsymmorphic symmetry in the momentum space of lattice models. Finally, we experimentally realize all aspects of their phenomenology in a photonic platform with synthetic momenta. Our work highlights the subtle but crucial interplay between the topology of quasiparticles and of their underlying manifold.

DOI: 10.1103/PhysRevLett.132.266601

Weyl fermions are massless particles of definite chirality allowed by the standard model of particle physics [1]. Although they remain elusive as high-energy particles, they can emerge as low-energy excitations in quantum systems [2–5], and their dispersion also appears in certain classical systems [6–11]. Such Weyl quasiparticles occur near band degeneracies, known as Weyl points, in the momentum space of three-dimensional lattices, and exhibit a number of unique properties: (1) as monopoles of Berry curvature, they carry an integer topological charge, the first Chern number, the sign of which defines their chirality [12,13]. They are therefore robust to perturbations, even some that break translational symmetry [14–16]. (2) A bulk-boundary correspondence associates Weyl points with Fermi arcs—dispersive surface states that connect Weyl points of opposite charges [17]. (3) In the presence of gauge fields, they can generate a violation of chiral charge conservation, a phenomenon known as the chiral anomaly [18].

Formulating lattice theories that describe Weyl fermions, or chiral fermions more broadly, imposes global constraints on their chirality. The most noteworthy example is the Nielsen–Ninomiya theorem, that asserts, under general assumptions of locality, Hermiticity, and translational invariance, that the net chirality of all Weyl fermions vanishes [19,20]. In lattice field theories, the Nielsen–Ninomiya theorem generates additional unwanted fermion species, leading to the important problem of fermion doubling [21,22]. Additionally, since condensed matter systems are often crystalline, this theorem applies and constrains the total Weyl-point chirality in the Brillouin zone to vanish. This, in turn, directly impacts physical observables, e.g., the spectrum and dispersion of Fermi arcs [23], the chirality of Landau levels under an applied magnetic field [18,24], and electromagnetic responses to circularly polarized light [25,26].

Several approaches for circumventing the Nielsen–Ninomiya theorem have been proposed, all of which violate one or more of its assumptions [27–37]; however, none have explored the role of the topology of the underlying manifold. Indeed, the strong constraint imposed by this no-go theorem ultimately results from the topological properties of the momentum-space fundamental domain, i.e., the toroidal Brillouin zone [38]. Here, we demonstrate that the notions of chirality and topology for Weyl points are fundamentally altered on nonorientable momentum-space manifolds. We show that, while an absolute notion of chirality of Weyl points becomes inherently ambiguous, a relative chirality still exists, and that nonorientability provides a natural setting for the Nielsen–Ninomiya theorem to be circumvented in an atypical fashion. We also show that Weyl points on nonorientable manifolds carry a $\mathbb{Z}_2$ topological charge and have an associated no-go

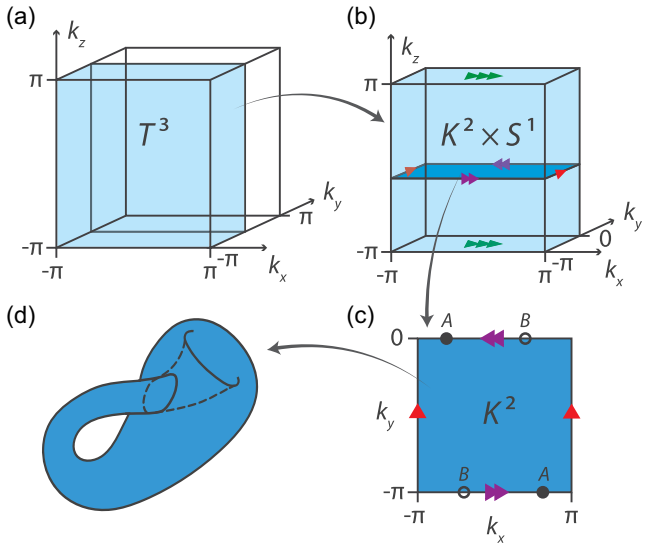

FIG. 1. (a) The momentum space of three-dimensional materials is typically represented as a torus, T^3. (b) In the case of Hamiltonians obeying the symmetry in Eq. (1), the fundamental domain in momentum space takes the form of a nonorientable manifold, $K^2 \times S^1$. The arrows indicate boundary identifications. (c) Two-dimensional cuts in the (k_x, k_y) plane form a Klein bottle, K^2. The Hamiltonian is identical at the pair of points labeled by A and B, and similarly along the entire $k_y = -\pi$ and $k_y = 0$ lines. (d) K^2 can be visualized as a closed manifold created by twisting and gluing one pair of opposing sides of a rectangle and gluing the other pair without a twist (as indicated by the arrows).

theorem that places global constraints on both the number of Weyl points and their total chirality. Finally, we experimentally realize such Weyl points in a photonic system endowed with synthetic momenta, paving the way to a wider exploration of the interplay between orientability and chirality.

We begin by discussing our scheme for obtaining Hamiltonians of lattice systems with nonorientable momentum-space manifolds. The Bloch Hamiltonian $H(\mathbf{k})$, in an appropriate basis, is invariant under translations by any reciprocal lattice vector $\mathbf{G}$, i.e., $H(\mathbf{k}) = H(\mathbf{k} + \mathbf{G})$. This reflects a redundancy in $\mathbf{k}$ space, since both $\mathbf{k}$ and $\mathbf{k} + \mathbf{G}$ label the same physical momentum point. By restricting $\mathbf{k}$ to the set of unique momenta, the Brillouin zone takes the form of a three-dimensional torus, denoted as T^3 (Fig. 1(a)). This toroidal nature of momentum space is unavoidable for a lattice.

Interestingly, under certain circumstances it is possible to subdivide the torus into closed manifolds that are nonorientable [39–43]. This can be achieved, e.g., by imposing a momentum-space glide symmetry on the Hamiltonian

$$H(k_x, k_y, k_z) = H(-k_x, k_y + \pi, k_z), \tag{1}$$

where we have set the lattice constant to unity. This symmetry leads to a further redundancy in $\mathbf{k}$ space, since the Hamiltonian, along with its eigenstates and energy spectrum, is identical at momenta (k_x, k_y, k_z) and $(-k_x, k_y + \pi, k_z)$. This symmetry operation subdivides the torus into two fundamental domains: without loss of generality we select the domain $-\pi \le k_x, k_z < \pi$ and $-\pi \le k_y < 0$ as their representative. The nonsymmorphic nature of the symmetry in Eq. (1) allows for boundary identifications to be made at the $k_y = 0$ and $k_y = -\pi$ planes in a twisted fashion [Fig. 1(b)], resulting in a closed manifold. The fundamental domain can consequently be expressed as the direct product of a nonorientable Klein bottle (K^2) in the (k_x, k_y) plane and a circle (S^1) in the k_z direction, i.e., $K^2 \times S^1$. The Klein bottle can be visualized by gluing one pair of opposite sides of a rectangle and twisting and gluing the other pair [Fig. 1(c)]. Figure 1(d) shows an immersion of a Klein bottle in $\mathbb{R}^3$.

We note that the direct equality in Eq. (1), without unitary conjugation of the Hamiltonian, is crucial [44], and distinguishes this symmetry from spatial symmetries, such as rotations, that subdivide the Brillouin zone into identical smaller copies, but which are open manifolds. This unitary-free symmetry is analogous to translational symmetry which reduces the domain of the Hamiltonian from $\mathbb{R}^3$ to T^3, leading to identical physics at the identified boundaries. In further contrast to spatial symmetries, the nonsymmorphic nature of this symmetry in momentum space leaves no momentum point invariant.

Next, we consider the consequences of this symmetry using a two-band, spinless model on the three-dimensional cubic lattice with a Bloch Hamiltonian of the form

$$H(\mathbf{k}) = \mathbf{d} \cdot \boldsymbol{\sigma} = d_x(\mathbf{k})\sigma_x + d_y(\mathbf{k})\sigma_y + d_z(\mathbf{k})\sigma_z, \tag{2}$$

where $\sigma_{x,y,z}$ are the Pauli matrices, and the components of $\mathbf{d}(\mathbf{k}) = [d_x, d_y, d_z](\mathbf{k})$ are individually subject to Eq. (1). As a concrete example, we take

$$\begin{aligned} d_x(\mathbf{k}) &= \cos k_x, \\ d_y(\mathbf{k}) &= \sin k_z - \sin k_x \sin k_y - \tfrac{1}{2}, \\ d_z(\mathbf{k}) &= \cos k_z + \sin k_x \cos k_y + 1 \end{aligned} \tag{3}$$

and note that, physically, the constraints on $\mathbf{d}(\mathbf{k})$ imply a suppression of certain hoppings in real space [45].

The bands touch at Weyl points where $|\mathbf{d}(\mathbf{k})| = 0$. For our model, we find two Weyl points in the $K^2 \times S^1$ fundamental domain [Fig. 2(a)]. Their chiralities can be computed by enclosing each Weyl point within a spherical shell and integrating the Berry curvature flux through it [46]. However, since $K^2 \times S^1$ is nonorientable, there is no globally consistent orientation. This is relevant for the calculation of the Chern number since it is a pseudoscalar,

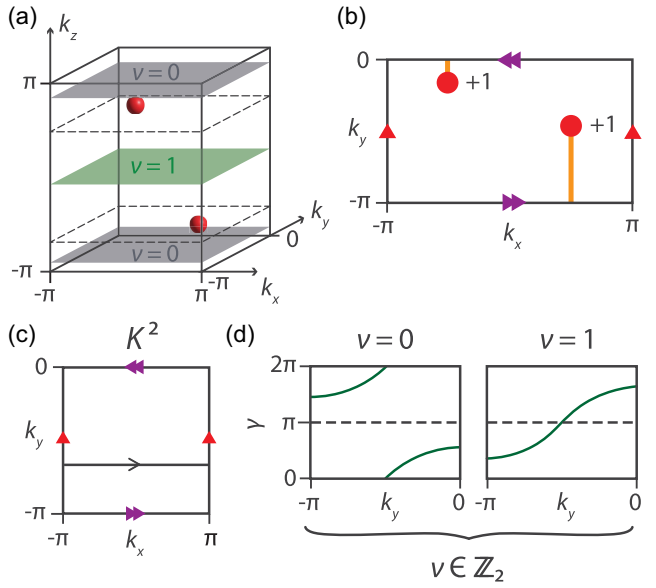

FIG. 2. (a) The distribution of Weyl points (red spheres) at $E = 0$ in the fundamental domain, $K^2 \times S^1$, for the model in Eq. (3). All Weyl points have Chern number $+1$. Highlighted k_z planes indicate that an odd number of Weyl points mediate the transitions between different values of the $\mathbb{Z}_2$ invariant ν, discussed below. (b) Fermi arcs obtained on truncating the system along the z direction, connecting projections of Weyl points (red circles) with charges of the same sign via an orientation-reversing path. The associated fundamental surface Brillouin zone forms a Klein bottle. (c) Berry phase γ calculated on the Klein bottle K^2. The Berry connection is integrated along k_x and plotted as a function of k_y from $-\pi$ to 0. (d) The invariant ν gives a $\mathbb{Z}_2$ classification on K^2, the transitions of which are mediated by Weyl points as shown in (a).

and therefore flips sign upon orientation reversal. Thus, while an absolute sign for the chirality cannot be established, an orientation choice can be made on any finite region that does not include the orientation-reversing planes $k_y = -\pi$ and $k_y = 0$, such that it contains all the Weyl points. This choice can be used to assign the signs of their charges through a Berry curvature flux integral, which provides an unambiguous definition of relative chirality within the region. Interestingly, this implies that nonorientability allows all Weyl points on the manifold to have the same relative chirality. For example, if we start with two Weyl points of opposite chiralities, we can change the chirality of one of them by moving it along an orientation-reversing path, i.e., one that crosses the planes $k_y = -\pi$ and $k_y = 0$ an odd number of times, resulting in both Weyl points having the same relative chirality. This is similar to the chirality flip observed in non-Hermitian systems when Weyl points encircle exceptional nodal lines [58,59].

In our model, we find that both Weyl points on the $K^2 \times S^1$ manifold carry a charge of $+1$ [Fig. 2(a)]. Evidently, the Nielsen–Ninomiya theorem is circumvented on the fundamental domain [60] since the total chirality is $\chi = +2$. In [45], we show that this circumvention is possible because $\mathbf{d}(\mathbf{k})$ is discontinuous on $K^2 \times S^1$, even though the Hamiltonian itself is continuous. This discontinuity is directly tied to the nonorientability of the underlying manifold, and renders the Nielsen–Ninomiya theorem inapplicable. We also further explore the nature of this circumvention in [45]: first, we show a direct physical consequence of this circumvention—systems that exhibit a nonzero total chirality on $K^2 \times S^1$ necessarily host gapless surface states where twisted boundary identifications are made; and second, we prove that fine-tuning $\mathbf{d}(\mathbf{k})$, such that it is continuous on the fundamental domain, restores the Nielsen–Ninomiya theorem.

Physically, the relative chiralities of Weyl points can also be ascertained through the Fermi arcs: Weyl points of the same chirality are connected via Fermi arcs that lie on orientation-reversing paths [Fig. 2(b)]; whereas Weyl points with opposite chirality are connected via Fermi arcs that lie on orientation-preserving paths, i.e., those that intersect the lines $k_y = -\pi$ and $k_y = 0$ an even number of times. In [45], we show that these features are general by considering a different nonorientable manifold, the real projective plane RP^2.

We will now show that Weyl points on nonorientable manifolds carry an additional $\mathbb{Z}_2$ topological charge, which results in a different no-go theorem. To identify the $\mathbb{Z}_2$ charge, we consider topological invariants on two-dimensional gapped subspaces of the three-dimensional Brillouin zone. Explicitly, we consider fixed-k_z subspaces restricted to the fundamental domain, which form Klein bottles, K^2 [Figs. 1(b) and 1(c)]. We can then integrate the Berry connection along the k_x direction to obtain the Berry phase $\gamma(k_y)$ [Fig. 2(c)]. Since $k_y = -\pi$ and $k_y = 0$ are related by a k_x-mirror operation, integrating the Berry connection along these lines leads to a relative minus sign, and therefore $\gamma(k_y = -\pi) = -\gamma(k_y = 0) \pmod{2\pi}$. By counting the number of crossings W_π of the Berry phase through the horizontal line $\gamma = \pi$, it can be shown that curves with a given W_π parity can be deformed into one another but cannot be deformed into those with a different parity. This defines a $\mathbb{Z}_2$ invariant $\nu \equiv W_\pi \bmod 2 \in \{0, 1\}$ on K^2 [39] [Fig. 2(d)]. Similar to the Chern number, ν originates from the topological classification of line bundles over their fundamental domains, which can be expressed in terms of the second cohomology groups $H^2(T^2; \mathbb{Z}) = \mathbb{Z}$ and $H^2(K^2; \mathbb{Z}) = \mathbb{Z}_2$. Therefore, the classification is stable under the addition of trivial bands. Furthermore, this invariant leads to edge states when interfaced with a trivial system [39,45].

We now compute the value of ν for various fixed-k_z, Klein-bottle cuts for the model in Eq. (3). Figure 2(a) shows that the value of $\nu(k_z)$ changes by unity as k_z passes through an odd number of Weyl points. This suggests that a nontrivial value of ν is associated with Weyl points of odd chirality. We show in [45] that a local Berry phase

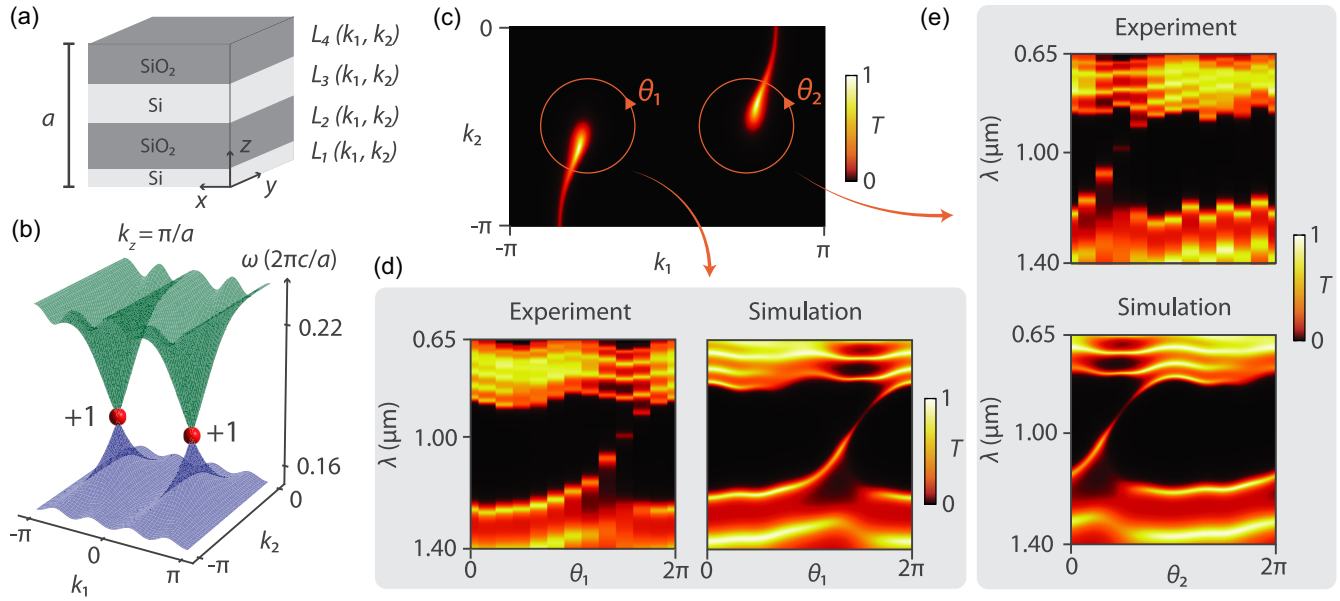

FIG. 3. (a) The unit cell of the PhCs that consist of four layers of thicknesses L_1 to L_4. The lattice constant in the z direction is a. (b) The lowest two bands of the PhCs at $k_z = \pi/a$, as a function of k_1 and k_2. The two Weyl points, shown as red spheres, both carry a Chern number of $+1$. These are "ideal" Weyl points that are frequency isolated from the other bands. (c) Fermi arcs on the top surface of the finite-in-z system on the K^2 surface Brillouin zone formed by the parameters k_1 and k_2. (d,e) Experimentally obtained and simulated transmission spectra showing the Fermi-arc surface state dispersion along circular loops enclosing the Weyl points. The loops around the projections of the Weyl points are parametrized by angular variables θ_1 and θ_2.

calculation for the $\mathbb{Z}_2$ invariant can be carried out by enclosing the Weyl point within a *two-sided* Klein bottle [47]. This shows that ν is indeed sourced by Weyl points and, accordingly, we may associate a $\mathbb{Z}_2$ charge to each. The same conclusion can be reached by relating ν to the Chern number C of the Weyl point by noticing that the Berry phase jumps by $2\pi C$ at the momentum of the Weyl point [48,49]. This leads to the relation $\nu = C \bmod 2$ [45].

Having uncovered that Weyl points carry a $\mathbb{Z}_2$ charge, we now show that this charge is subject to a no-go theorem on $K^2 \times S^1$. The argument proceeds as follows: since the k_z direction is periodic, $\nu(k_z = -\pi) = \nu(k_z = \pi)$. This forbids the presence of a net nonzero $\mathbb{Z}_2$ charge of the Weyl points within $K^2 \times S^1$. To show this, we consider the case of a single Weyl point at the $k_z = 0$ plane. Because of this Weyl point, the value of $\nu(k_z = 0^-)$ would differ from $\nu(k_z = 0^+)$ by unity. If there are no other Weyl points, it follows that the values $\nu(k_z = -\pi) = \nu(k_z = 0^-)$ and $\nu(k_z = \pi) = \nu(k_z = 0^+)$ would not be equal, which is not possible if the k_z direction is periodic. Thus, a second Weyl point is needed to ensure that the invariants at the two k_z planes match. Accordingly, the total $\mathbb{Z}_2$ charge of the Weyl points on $K^2 \times S^1$ must vanish; or, equivalently, the sum of Chern numbers of the Weyl points must be even—but as we have shown, not necessarily vanishing. This no-go theorem implies that for systems obeying Eq. (1) the minimum number of singly charged Weyl points is two on $K^2 \times S^1$, and four on the toroidal Brillouin zone, even under broken time-reversal symmetry. In [45], we further discuss the roles of inversion and time-reversal symmetries, and provide a second argument for this no-go theorem based on the configuration of Fermi arcs.

In this final section, we turn our attention to an experimental demonstration of Weyl points on nonorientable manifolds, which we realize in a photonic system endowed with synthetic momenta. The system considered here consists of a family of optical multilayer structures, i.e., one-dimensional photonic crystals (PhCs). Their unit cells are composed of four dielectric layers alternating between two materials, silicon ($\varepsilon_{\mathrm{Si}} = 12.5$) and SiO_2 ($\varepsilon_{\mathrm{SiO_2}} = 2.25$), with a lattice constant a in the z direction [Fig. 3(a)]. Light propagation in such PhCs is governed by a Maxwell eigenvalue problem for the electromagnetic field eigenmodes, and their corresponding frequency eigenvalues, analogous to electrons moving in a crystalline solid [61,62]. When light propagation along the z direction is considered, this is reduced to a one-dimensional problem which is solved using Bloch's theorem. The resulting field solutions form discrete frequency bands as a function of the quasimomentum k_z, which may be separated by photonic band gaps.

We introduce two periodic parameters, k_1 and k_2, to modulate the thicknesses, L_1, L_2, L_3, and L_4, of each of the four layers in the unit cell. The parameters k_1, k_2 serve as synthetic momentum degrees of freedom which, along with the quasimomentum k_z, result in a three-dimensional toroidal parameter space within which Weyl points can exist [36,63,64]. We choose L_1 to L_4

such that the nonsymmorphic symmetry given in Eq. (1) is satisfied in (k_1, k_2, k_z) space. In particular, we choose $L_1 = \frac{1}{4}a(1+\cos k_1)$, $L_2 = \frac{1}{4}a(1+\sin k_1 \cos k_2)$, $L_3 = \frac{1}{4}a(1-\cos k_1)$, $L_4 = \frac{1}{4}a(1-\sin k_1 \cos k_2)$. Thus the fundamental domain is $K^2 \times S^1$ after making boundary identifications at the $k_2 = -\pi$ and 0 planes.

We find that the fundamental domain hosts two Weyl points between the lowest two bands of this system [Fig. 3(b)], each with a relative chirality of $+1$. This implies that they each carry a $\mathbb{Z}_2$ charge of $\nu = 1$, as we explicitly show in [45]. The total chirality of the Weyl points therefore does not vanish, similar to what was observed in the tight-binding model in Eq. (3). However, the total $\mathbb{Z}_2$ charge vanishes, consistent with the no-go theorem for these charges. The higher bands can host increasingly larger numbers of Weyl points, while always maintaining a vanishing total $\mathbb{Z}_2$ charge. We discuss the many-band case in more detail in [45].

On truncating the PhCs along the z direction, Fermi arcs are expected to emerge from the projections of the Weyl points in the surface Brillouin zone formed by (k_1, k_2). Since the Fermi arcs are localized on the surfaces, they possess an enormous linewidth generated by the strong out-coupling to plane waves in the air above the PhCs. To remedy this, we clad the PhCs with additional layers on the top surface to better confine these states [45]. Doing so allows for the observation of the Fermi arcs in the transmission spectrum of the PhCs, a simulation of which is shown in Fig. 3(c). When the dispersion of the Fermi arcs is plotted along a loop that encloses the projection of a Weyl point, these states fully cross the band gap, with the direction of their spectral flow determined by the sign of the chirality of the enclosed Weyl point. Since our Weyl points have the same chirality, we expect the same spectral flow pattern for both nodes as simulated in Figs. 3(d) and 3(e).

For the experiment, we fabricate a series of PhCs that correspond to values of k_1 and k_2 lying on the loops that enclose the Weyl point projections, as shown in Fig. 3(c) (further details on the simulations and experiment are given in [45]). Figures 3(d) and 3(e) show the experimental results along with corresponding simulations. We see that the surface states cross the gap with identical spectral flow for both Weyl points, indicating that they carry the same chirality.

In summary, by implementing Weyl quasiparticles in lattice models with nonsymmorphic momentum-space symmetries, we have explored their fate on nonorientable manifolds. On the associated fundamental domain, the Hamiltonian, its eigenstates, and all physical observables are continuous. However, we have shown that the chirality of Weyl points need not sum to zero, circumventing the Nielsen–Ninomiya theorem. The underlying nonorientable domain endows the Weyl points with an additional $\mathbb{Z}_2$ charge, whose conservation enforces a new no-go theorem. Finally, we have experimentally demonstrated the phenomenology of such Weyl points in a photonic platform with synthetic momenta. Our work suggests several new research directions. For example, one can consider other nonorientable manifolds in dimensions two and higher that might host their own unique topological invariants and new gapless points [65–67]. It will also be interesting to explore the properties of Landau levels originating from both real and pseudomagnetic fields when the chirality does not vanish [24,68–70]. More broadly, this opens up new avenues to explore how other chiral objects, such as multifold fermions [12,71] and exceptional points [37,72], fare in nonorientable settings. We believe that the approaches introduced here may help answer these fundamental questions.

We thank Clifford Taubes, Terry A. Loring, Adolfo G. Grushin, and Jonathan Guglielmon for stimulating discussions. A. G. F. acknowledges support from the Henry W. Kendall Fellowship and the Whiteman Fellowship, and thanks the University of São Paulo for its hospitality, where part of this work was completed. T. C. acknowledges the support of a research grant (Project No. 42106) from Villum Fonden. S. V., M. C. R., T. L. H., and M. S. acknowledge support from the U.S. Office of Naval Research (ONR) Multidisciplinary University Research Initiative (MURI) under Grant No. N00014-20-1-2325 on Robust Photonic Materials with Higher-Order Topological Protection. This material is based upon work also supported in part by the U.S. Army Research Office through the Institute for Soldier Nanotechnologies at MIT, under Collaborative Agreement No. W911NF-23-2-0121. This work was carried out in part through the use of MIT.nano's facilities.

*These authors contributed equally to this work.
†agfons@mit.edu
‡svaidya1@mit.edu

[1] H. Weyl, Elektron und Gravitation. I, Z. Phys. **56**, 330 (1929).
[2] S. Y. Xu, I. Belopolski, N. Alidoust, M. Neupane, G. Bian, C. Zhang, R. Sankar, G. Chang, Z. Yuan, C. C. Lee *et al.*, Discovery of a Weyl fermion semimetal and topological Fermi arcs, Science **349**, 613 (2015).
[3] B. Q. Lv, H. M. Weng, B. B. Fu, X. P. Wang, H. Miao, J. Ma, P. Richard, X. C. Huang, L. X. Zhao, G. F. Chen *et al.*, Experimental discovery of Weyl semimetal TaAs, Phys. Rev. X **5**, 031013 (2015).
[4] N. P. Armitage, E. J. Mele, and A. Vishwanath, Weyl and Dirac semimetals in three-dimensional solids, Rev. Mod. Phys. **90**, 015001 (2018).
[5] Z.-Y. Wang, X.-C. Cheng, B.-Z. Wang, J.-Y. Zhang, Y.-H. Lu, C.-R. Yi, S. Niu, Y. Deng, X.-J. Liu, S. Chen *et al.*, Realization of an ideal Weyl semimetal band in a quantum gas with 3D spin-orbit coupling, Science **372**, 271 (2021).

[6] L. Lu, Z. Wang, D. Ye, L. Ran, L. Fu, J. D. Joannopoulos, and M. Soljačić, Experimental observation of Weyl points, Science **349**, 622 (2015).
[7] F. Li, X. Huang, J. Lu, J. Ma, and Z. Liu, Weyl points and Fermi arcs in a chiral phononic crystal, Nat. Phys. **14**, 30 (2018).
[8] H. He, C. Qiu, X. Cai, M. Xiao, M. Ke, F. Zhang, and Z. Liu, Observation of quadratic Weyl points and double-helicoid arcs, Nat. Commun. **11**, 1820 (2020).
[9] J. Noh, S. Huang, D. Leykam, Y. D. Chong, K. P. Chen, and M. C. Rechtsman, Experimental observation of optical Weyl points and Fermi arc-like surface states, Nat. Phys. **13**, 611 (2017).
[10] S. Vaidya, J. Noh, A. Cerjan, C. Jörg, G. von Freymann, and M. C. Rechtsman, Observation of a charge-2 photonic Weyl point in the infrared, Phys. Rev. Lett. **125**, 253902 (2020).
[11] C. Jörg, S. Vaidya, J. Noh, A. Cerjan, S. Augustine, G. von Freymann, and M. C. Rechtsman, Observation of quadratic (charge-2) Weyl point splitting in near-infrared photonic crystals, Laser Photonics Rev. **16**, 2100452 (2022).
[12] B. Bradlyn, J. Cano, Z. Wang, M. Vergniory, C. Felser, R. J. Cava, and B. A. Bernevig, Beyond Dirac and Weyl fermions: Unconventional quasiparticles in conventional crystals, Science **353**, aaf5037 (2016).
[13] G. Chang, B. J. Wieder, F. Schindler, D. S. Sanchez, I. Belopolski, S.-M. Huang, B. Singh, D. Wu, T.-R. Chang, T. Neupert *et al.*, Topological quantum properties of chiral crystals, Nat. Mater. **17**, 978 (2018).
[14] J. H. Pixley, J. H. Wilson, D. A. Huse, and S. Gopalakrishnan, Weyl semimetal to metal phase transitions driven by quasiperiodic potentials, Phys. Rev. Lett. **120**, 207604 (2018).
[15] A. G. Fonseca, T. Christensen, J. D. Joannopoulos, and M. Soljačić, Quasicrystalline Weyl points and dense Fermi–Bragg arcs, Phys. Rev. B **108**, L121109 (2023).
[16] V. Mastropietro, Stability of Weyl semimetals with quasi-periodic disorder, Phys. Rev. B **102**, 045101 (2020).
[17] X. Wan, A. M. Turner, A. Vishwanath, and S. Y. Savrasov, Topological semimetal and Fermi-arc surface states in the electronic structure of pyrochlore iridates, Phys. Rev. B **83**, 205101 (2011).
[18] H. B. Nielsen and M. Ninomiya, The Adler–Bell–Jackiw anomaly and Weyl fermions in a crystal, Phys. Lett. **130B**, 389 (1983).
[19] H. B. Nielsen and M. Ninomiya, Absence of neutrinos on a lattice: (I). Proof by homotopy theory, Nucl. Phys. B **185**, 20 (1981).
[20] H. B. Nielsen and M. Ninomiya, Absence of neutrinos on a lattice: (II). Intuitive topological proof, Nucl. Phys. B **193**, 173 (1981).
[21] M. Luscher, Chiral gauge theories revisited, Subnucl. Ser. **38**, 41 (2002).
[22] D. B. Kaplan, Chiral symmetry and lattice fermions, arXiv:0912.2560.
[23] M. Z. Hasan, S.-Y. Xu, I. Belopolski, and S.-M. Huang, Discovery of Weyl fermion semimetals and topological Fermi arc states, Annu. Rev. Condens. Matter Phys. **8**, 289 (2017).
[24] R. Ilan, A. G. Grushin, and D. I. Pikulin, Pseudo-electromagnetic fields in 3D topological semimetals, Nat. Rev. Phys. **2**, 29 (2020).
[25] S. Sekh and I. Mandal, Circular dichroism as a probe for topology in three-dimensional semimetals, Phys. Rev. B **105**, 235403 (2022).
[26] F. de Juan, A. G. Grushin, T. Morimoto, and J. E. Moore, Quantized circular photogalvanic effect in Weyl semimetals, Nat. Commun. **8**, 15995 (2017).
[27] H. Neuberger, Exactly massless quarks on the lattice, Phys. Lett. B **417**, 141 (1998).
[28] P. Hernandez, K. Jansen, and M. Luscher, Locality properties of Neuberger's lattice Dirac operator, Nucl. Phys. B **552**, 363 (1999).
[29] P. H. Ginsparg and K. G. Wilson, A remnant of chiral symmetry on the lattice, Phys. Rev. D **25**, 2649 (1982).
[30] D. B. Kaplan, A method for simulating chiral fermions on the lattice, Phys. Lett. B **288**, 342 (1992).
[31] J. Wang and Y.-Z. You, Symmetric mass generation, Symmetry **14**, 1475 (2022).
[32] M. S. Rudner, N. H. Lindner, E. Berg, and M. Levin, Anomalous edge states and the bulk-edge correspondence for periodically driven two-dimensional systems, Phys. Rev. X **3**, 031005 (2013).
[33] Z.-M. Yu, W. Wu, Y. X. Zhao, and S. A. Yang, Circumventing the no-go theorem: A single Weyl point without surface Fermi arcs, Phys. Rev. B **100**, 041118(R) (2019).
[34] J. Ahn, S. Park, and B.-J. Yang, Failure of Nielsen–Ninomiya theorem and fragile topology in two-dimensional systems with space-time inversion symmetry: Application to twisted bilayer graphene at magic angle, Phys. Rev. X **9**, 021013 (2019).
[35] A. Bouhon, Q. Wu, R.-J. Slager, H. Weng, O. V. Yazyev, and T. Bzdušek, Non-Abelian reciprocal braiding of Weyl points and its manifestation in ZrTe, Nat. Phys. **16**, 1137 (2020).
[36] Q. Wang, M. Xiao, H. Liu, S. Zhu, and C. T. Chan, Optical interface states protected by synthetic Weyl points, Phys. Rev. X **7**, 031032 (2017).
[37] J. L. K. König, K. Yang, J. C. Budich, and E. J. Bergholtz, Braid-protected topological band structures with unpaired exceptional points, Phys. Rev. Res. **5**, L042010 (2023).
[38] L. H. Karsten, Lattice fermions in Euclidean space-time, Phys. Lett. **104B**, 315 (1981).
[39] Z. Y. Chen, S. A. Yang, and Y. X. Zhao, Brillouin Klein bottle from artificial gauge fields, Nat. Commun. **13**, 2215 (2022).
[40] Y. Wang, C. Zhang, Z. Y. Chen, B. Liang, Y. X. Zhao, and J. Cheng, Chess-board acoustic crystals with momentum-space nonsymmorphic symmetries, arXiv:2305.07174.
[41] Z. Zhu, L. Yang, J. Wu, Y. Meng, X. Xi, B. Yan, J. Chen, J. Lu, X. Huang, W. Deng *et al.*, Brillouin Klein space and half-turn space in three-dimensional acoustic crystals, arXiv:2305.08450.
[42] C. Zhang, Z. Y. Chen, Z. Zhang, and Y. X. Zhao, General theory of momentum-space nonsymmorphic symmetry, Phys. Rev. Lett. **130**, 256601 (2023).
[43] T. Morimoto, H. C. Po, and A. Vishwanath, Floquet topological phases protected by time glide symmetry, Phys. Rev. B **95**, 195155 (2017).

[44] In [45], we discuss how Eq. (1) is modified if the orbital degrees of freedom are spatially displaced from the origin in the unit cell.
[45] See Supplemental Material at http://link.aps.org/supplemental/10.1103/PhysRevLett.132.266601 for more details, which includes Refs. [38,39,46–57].
[46] D. Vanderbilt, *Berry Phases in Electronic Structure Theory: Electric Polarization, Orbital Magnetization and Topological Insulators* (Cambridge University Press, Cambridge, England, 2018).
[47] J. W. Woll, Jr., One-sided surfaces and orientability, Two-Year Coll. Math. J. **2**, 5 (1971).
[48] H. Yoshida, T. Zhang, and S. Murakami, Polarization jumps by breaking symmetries of two-dimensional Weyl semimetals, Phys. Rev. B **107**, 035122 (2023).
[49] H. Yoshida, T. Zhang, and S. Murakami, Polarization jumps across topological phase transitions in two-dimensional systems, Phys. Rev. B **108**, 075160 (2023).
[50] J. Cayssol and J. N. Fuchs, Topological and geometrical aspects of band theory, J. Phys. Mater. **4**, 034007 (2021).
[51] A. Hatcher, *Algebraic Topology* (Cambridge University Press, Cambridge, England, 2001).
[52] B. A. Bernevig and T. L. Hughes, *Topological Insulators and Topological Superconductors* (Princeton University Press, Princeton, NJ, 2013).
[53] K. Shiozaki, M. Sato, and K. Gomi, Z_2 topology in nonsymmorphic crystalline insulators: Möbius twist in surface states, Phys. Rev. B **91**, 155120 (2015).
[54] E. Witten, Three lectures on topological phases of matter, Riv. Nuovo Cimento **39**, 313 (2016).
[55] J. W. Milnor and J. D. Stasheff, *Characteristic Classes* (Princeton University Press, Princeton, NJ, 1974).
[56] V. Liu and S. Fan, S^4: A free electromagnetic solver for layered periodic structures, Comput. Phys. Commun. **183**, 2233 (2012).
[57] S. G. Johnson and J. D. Joannopoulos, Block-iterative frequency-domain methods for Maxwell's equations in a planewave basis, Opt. Express **8**, 173 (2001).
[58] X.-Q. Sun, C. C. Wojcik, S. Fan, and T. Bzdušek, Alice strings in non-Hermitian systems, Phys. Rev. Res. **2**, 023226 (2020).
[59] C. C. Wojcik, X.-Q. Sun, T. Bzdušek, and S. Fan, Homotopy characterization of non-Hermitian Hamiltonians, Phys. Rev. B **101**, 205417 (2020).
[60] We note that the total chirality on T^3 is vanishing and therefore the Nielsen–Ninomiya theorem holds on T^3 even if it is violated on $K^2 \times S^1$.
[61] J. D. Joannopoulos, S. G. Johnson, J. N. Winn, and R. D. Meade, *Photonic Crystals: Molding the Flow of Light* (Princeton University Press, Princeton, NJ, 2008).
[62] K. Sakoda, *Optical Properties of Photonic Crystals*, 2nd ed., Springer Series in Optical Sciences Vol. 80 (Springer, New York, 2005).
[63] D. H.-Minh. Nguyen, C. Devescovi, D. X. Nguyen, H. S. Nguyen, and D. Bercioux, Fermi arc reconstruction in synthetic photonic lattice, Phys. Rev. Lett. **131**, 053602 (2023).
[64] D. Kim, A. Baucour, Y.-S. Choi, J. Shin, and M.-K. Seo, Spontaneous generation and active manipulation of real-space optical vortices, Nature (London) **611**, 48 (2022).
[65] Y.-L. Tao, M. Yan, M. Peng, Q. Wei, Z. Cui, S. A. Yang, G. Chen, and Y. Xu, Higher-order Klein bottle topological insulator in three-dimensional acoustic crystals, Phys. Rev. B **109**, 134107 (2024).
[66] H. Jinbing, Z. Songlin, and Y. Yi, Synthetic gauge fields enable high-order topology on Brillouin real projective plane, Phys. Rev. Lett., **132**, 213801 (2024).
[67] C.-A. Li, J. Sun, S.-B. Zhang, H. Guo, and B. Trauzettel, Klein-bottle quadrupole insulators and Dirac semimetals, Phys. Rev. B **108**, 235412 (2023).
[68] J. Behrends, S. Roy, M. H. Kolodrubetz, J. H. Bardarson, and A. G. Grushin, Landau levels, Bardeen polynomials, and Fermi arcs in Weyl semimetals: Lattice-based approach to the chiral anomaly, Phys. Rev. B **99**, 140201(R) (2019).
[69] M. Barsukova, F. Grisé, Z. Zhang, S. Vaidya, J. Guglielmon, M. I. Weinstein, L. He, B. Zhen, R. McEntaffer, and M. C. Rechtsman, Direct observation of Landau levels in silicon photonic crystals, Nat. Photonics **18**, 580 (2024).
[70] R. Barczyk, L. Kuipers, and E. Verhagen, Observation of Landau levels and chiral edge states in photonic crystals through pseudomagnetic fields induced by synthetic strain, Nat. Photonics **18**, 574 (2024).
[71] J. L. Mañes, Existence of bulk chiral fermions and crystal symmetry, Phys. Rev. B **85**, 155118 (2012).
[72] E. J. Bergholtz, J. C. Budich, and F. K. Kunst, Exceptional topology of non-Hermitian systems, Rev. Mod. Phys. **93**, 015005 (2021).